Effect of $BaZrO_3$ Addition and Film Growth on Superconducting Properties of $(Nd, Eu, Gd)Ba_2Cu_3O_y$ Thin Films

Yusuke Ichino, Yutaka Yoshida, Kouichi Inoue, Toshinori Ozaki, Yoshiaki Takai, Kaname Matsumoto, Masashi Mukaida, Ryusuke Kita, Ataru Ichinose, and Shigeru Horii

***Abstract*—We report that $(Nd, Eu, Gd)Ba_2Cu_3O_y$ (NEG) films grown by low temperature growth (LTG) technique exhibit excellent superconducting properties in magnetic fields. In this study, we aim to improve the superconducting properties of NEG films by means of a modified LTG technique (mLTG) in which the surface of a highly c-axis oriented NEG seed layer is decorated by $BaZrO_3$ (BZO) nanodots and an NEG upper layer on the seed layer is deposited at relatively low substrate temperature by using a BZO doped NEG123 target. From magnetic field and angular dependence of J_c, even J_c peak around $B//c$-axis of an LTG-NEG films including BZO was larger than that of LTG-NEG without BZO. Furthermore, the mLTG-NEG films showed larger J_c peak than the LTG-NEG films with BZO and the J_c peak increased with increasing the BZO nanodots density. TEM images clarified that these films included BZO nanorods with a diameter of 5$\sim$10 nm and the number density increased by introducing the BZO nanodots. Therefore, we concluded that the mLTG enabled to improve the superconducting properties due to control the configuration of BZO nanorods in the films.**

***Index Terms*—Flux pinning, high-temperature superconductors, low temperature growth technique, $REBa_2Cu_3O_y$ film.**

I. Introduction

FOR an enhancement of superconducting properties of $REBa_2Cu_3O_y$ (RE123, RE = Y, Sm, Nd and lanthanide) films, we have developed a novel thin film growth technique [1], [2]. The technique is named "low temperature growth (LTG)" technique and is consisted of two steps as shown in Fig. 1(a). Firstly, a c-axis oriented thin RE123 "seed" layer is grown on a substrate at a high substrate temperature by pulsed laser deposition (PLD). Second step is PLD deposition of a RE123 "upper" layer on the seed layer at relatively low substrate temperature. A Sm123 films fabricated by the LTG technique exhibited excellent superconducting properties in magnetic fields [3], [4]. Additionally, because of high critical current density (J_c) in $(Nd, Eu, Gd)Ba_2Cu_3O_y$ (NEG) melt textured bulk [5], we have fabricated NEG films by using the LTG technique and reported the excellent superconducting properties in magnetic fields [6].

Recently, a dramatic enhancement of flux pinning in Y123 films has been established by doping $BaZrO_3$ (BZO) into the films [7]. The doped BZO forms a lot of nanorods (NRs) along the Y123 [001] direction and with a diameter of a few nanometers. These BZO NRs act as c-axis correlated pinning centers. For further improvement of superconducting properties, it is needed to increase the BZO NRs density and to decrease the diameter as small as the coherence length of RE123. However, a formation mechanism of BZO NRs has not been clarified yet.

In this report, we introduced BZO nanodots (NDs) before a RE123 film growth in order to control BZO NR.

II. Experimental Procedure

NEG films were deposited on MgO(100) substrates by PLD method using KrF excimer laser and $Nd_{1/3}Eu_{1/3}Gd_{1/3}Ba_2Cu_3O_y$ sintered bulk as a target. The conditions are as follows: a target-substrate distance, 60 mm; a laser repetition rate, 10 Hz; a laser energy density, 3 J/cm^2; O_2 pressure, 1 Torr. In the deposition, a "pure" NEG and a 2 vol.% BZO doped NEG sintered targets were used.

In the case of LTG technique, seed layer with a thickness of $\sim$100 nm is deposited on substrates at a substrate temperature (T_s) of 870°C and then an upper layer with a thickness of $\sim$400 nm on the seed layer were deposited at T_s of 780 $\sim$ 840°C. In this case, the seed layer is deposited by using the pure NEG target, while either the pure or the BZO 2 vol.% doped NEG target is used for the deposition of the upper layer. In this paper, when an LTG-NEG film of which the upper layer is fabricated by using the BZO doped NEG target is described as LTG-NEG+BZO. Additionally, when a seed layer is decorated by BZO NDs, we call the process as modified LTG (mLTG). In the mLTG, the BZO NDs were formed by ablating the BZO target by a few laser pulses as shown in Figs. 1(b) and 1(c). The

Manuscript received August 15, 2008. First published June 30, 2009; current version published July 15, 2009. This work was supported in part by CREST of JST and by Grant-in-Aid for Scientific Research 19676005 and 20686065.

Y. Ichino, Y. Yoshida, K. Inoue, T. Ozaki and Y. Takai are with the Department of Energy Engineering and Science, Nagoya University, Furo-cho, Chikusa-ku, Nagoya 464-8603, Japan (e-mail: ichino@nuee.nagoya-u.ac.jp; yoshida@nuee.nagoya-u.ac.jp; k-inoue@ees.nagoya-u.ac.jp; ozaki_t@nuee.nagoya-u.ac.jp; takai@nuee.nagoya-u.ac.jp).

K. Matsumoto is with the Department of Materials Science, Kyushu Institute of Technology, 1-1 Sensui-cho, Tobata-ku, Kitakyushu-shi, Fukuoka, 804-8550, Japan (e-mail: matsu@post.matsc.kyutech.ac.jp).

M. Mukaida is with the Department of Materials Science and Engineering, Kyushu University, Hakozaki 6-10-1, Higashi-ku, Fukuoka 812-8581, Japan (e-mail: mukaida@zaiko.kyushu-u.ac.jp).

R. Kita is with the Graduate School of Science and Technology, Nanomaterials Section, 3-5-1 Johoku, Hamamatsu-shi 432-8561, Japan (e-mail: terkita@ipc.shizuoka.ac.jp).

A. Ichinose is with the Central Research Institute of Electric Power Industry, Yokosuka, Kanagawa 201-8511, Japan (e-mail: ai@criepi.denken.or.jp).

S. Horii is with the Department of Applied Chemistry, University of Tokyo, Hongo 7-3-1, Bunkyo-ku, Tokyo 113-8656, Japan (e-mail: tholy@mail.ecc.u-tokyo.ac.jp).

Color versions of one or more of the figures in this paper are available online at http://ieeexplore.ieee.org.

Digital Object Identifier 10.1109/TASC.2009.2018207

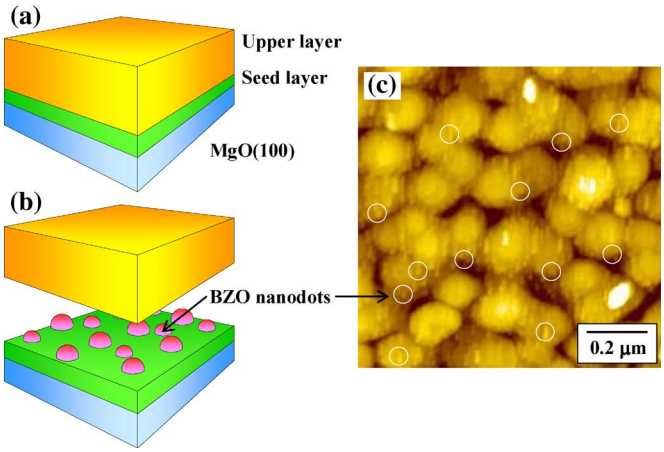

Fig. 1. Schematics of (a) LTG technique and (b) modified LTG technique. (c) An image of BZO nanodots observed by atomic force microscopy, which were grew up by 40 laser pulses using BZO target, on an NEG seed layer. A few BZO nanodots are enclosed with circle.

number density increased with increasing the pulses and the typical number density was a few hundreds per 1 μm square. In this paper, the films prepared by this technique were notated as $\mathrm{mLTG{-}NEG} + \mathrm{BZO}(n)$ in which n corresponds to the laser pulse number for the formation of BZO NDs.

The crystal structure and in-plane alignment of NEG films were examined by $2\theta{-}\omega$ scan and ϕ scan of X-ray diffraction (XRD) with Cu-Kα source. An a-axis grain mixed ratio of the films was calculated from an XRD peak intensity ratio of 200 to 005 reflections. Superconducting properties of the NEG films were measured by standard four-probe method. Microstructures of the films were observed by using cross sectional transmission electron microscopy (TEM).

III. Results and Discussion

A. Orientation, Crystallinity, and Critical Temperature

We checked orientation and crystallinity of the films against the density of the BZO NDs. Here, the crystallinity means a full width at half maximum (FWHM) of NEG 005 rocking curve. Fig. 2 shows a typical XRD pattern of an mLTG-NEG+BZO film. One can see that an epitaxial relationship between the NEG and substrate is (001)[100] NEG//(001)[100] MgO substrate. Even though the BZO NDs increased, these patterns did not change. However, the FWHMs of NEG 005 rocking curves in both the LTG-NEG+BZO and the mLTG-NEG+BZO films are degraded, compared to "pure" LTG-NEG film. For a "pure" LTG-NEG film without BZO content, the FWHM is about 0.06°. On the contrary, the FWHMs of the LTG- and the mLTG-NEG+BZO films were $0.10 \sim 0.15°$ and these values were independent of the BZO ND density on the seed layer. When we take into account that a deterioration of crystallinity is caused by a strain between BZO and RE123, a crystallinity of a RE123 film is degraded by increasing the BZO volume fraction. Thus, we can consider that the BZO volume fractions in our films are almost same in spite of the density of the BZO NDs. In other words, the BZO NDs do not diffuse into the NEG matrix.

Critical temperatures (T_cs) of the films including BZO were 89.7∼91.5 K and the values were also independent of the density of the BZO NDs. On the other hand, the pure LTG-NEG film shows 92.5 K. The lowering T_c of the films including the BZO would also originate from the crystal lattice deformation due to the strain between the BZO and the NEG.

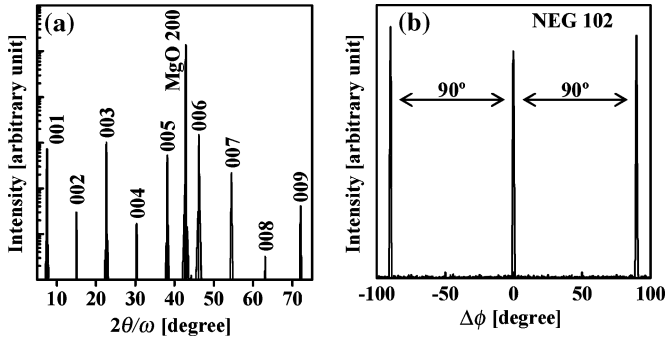

Fig. 2. Typical XRD patterns of an mLTG-NEG+BZO film. (a) $2\theta{-}\omega$ scan (out-of-plane texture) and (b) θ scan of NEG 102 reflection (in-plane texture).

B. Critical Current Density in Magnetic Fields

We evaluated critical current densities (J_cs) of the NEG films in magnetic fields applied parallel to the c-axis of the films and the result is exhibited in Fig. 3(a). One can see that J_cs at low fields (<6 T) of the BZO doped films were higher than that of the pure LTG-NEG film. This improvement is caused by an enhancement of the flux pinning force by introducing the BZO and this fact is same with other report, for example [7]. Especially, at the low fields, the mLTG-NEG+BZO(80) film exhibited the highest J_c in the films and there was a broad J_c peak around 1 T. However, J_cs of the films at high fields were lower than that of the pure LTG-NEG film. Therefore, BZO doping into NEG films at given doping level is not effective to improve the pinning at high magnetic fields higher than 6 T and more detailed investigation about higher doping level is required.

As mentioned in the previous section, the BZO NDs should not diffuse into the NEG matrix. Namely, the volume fraction of the BZO, which contributes to a formation of any microstructure made of BZO, should be independent of the BZO ND density. Therefore, we can think that the BZO NDs affect a pinning center consisted of BZO. In next section, we will discuss the BZO configuration in the films.

Next, anisotropy of the J_c against a magnetic field applied angle is investigated. Fig. 3(b) shows J_cs of the films as a function of the magnetic field applied angle. The magnitude of the magnetic field was 1 T at which the remarkable J_c enhancement in the mLTG-NEG+BZO(80) film was obtained (see Fig. 3(a)). Note the J_c around $B//c$-axis of the films, the J_c of the mLTG-NEG+BZO(80) film was the highest among the films in this study and the LTG-NEG+BZO film exhibited high J_c in the second. These facts mean that a high density c-axis correlated pinning centers exist in the films including BZO and the density is enhanced by the BZO NDs.

C. Microstructure

In this section, we investigated the microstructure of the films. Figs. 4(a) and 4(b) exhibit TEM images of the mLTG-NEG+BZO(80) and the LTG-NEG+BZO films, respec-

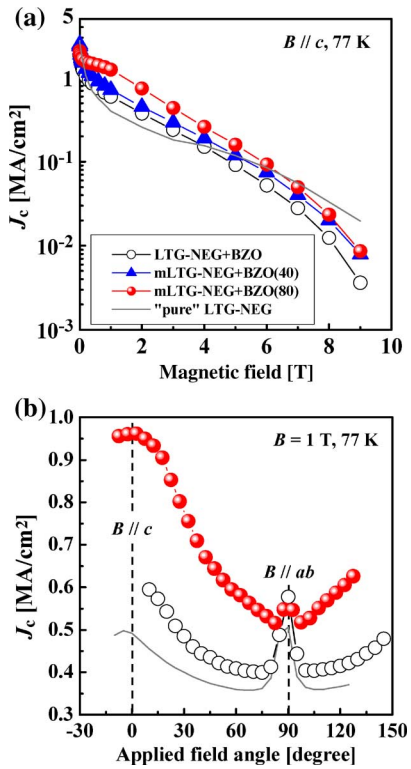

Fig. 3. Critical current density of NEG films at 77 K. (a) magnetic field dependence of J_c and (b) J_c in 1 T as a function of applied magnetic field angle. Same symbols are used in both (a) and (b).

tively. We found that the BZO NRs were embedded in the NEG matrix and the NRs grew along the NEG [001] direction, although the NRs somewhat tilt against the [001] direction. The existence of the BZO NRs is consistent with the result of the applied field angular dependence of J_c. Furthermore, one can see that a diameter of the BZO NRs in the mLTG-NEG+BZO(80) film was finer than that in the LTG-NEG+BZO film. Because the BZO content in the films should be the same and the BZO NDs in the mLTG-NEG+BZO(80) film do not diffuse into the NEG matrix, the fine NRs in the mLTG-NEG+BZO(80) film means an increase of the number density of BZO NRs. For a confirmation of the increase, we made a diameter-histogram of the BZO NRs in the films as shown in Fig. 4(c). The diameter distribution is classified into two groups in this figure. One is a group of the diameter less than 10 nm and another one is a group of the diameter more than 10 nm. In the case of the LTG-NEG+BZO film, diameter of a BZO NR belonged to either group. However, the greater part of the BZO NRs in the mLTG-NEG+BZO(80) film was in the group of small diameter. This fact means that the BZO NDs prevented a growth of coarse BZO NR. Although this detailed mechanism is under considering, the nucleation of the BZO NRs may be encouraged by the underlying BZO NDs due to a low interfacial energy between the BZO nucleus and the BZO NDs. Namely, because it is easy to grow BZO on the BZO NDs, we suggest that the BZO NRs directly grow on the BZO NDs. As a result, the number density increased and the diameter decreased.

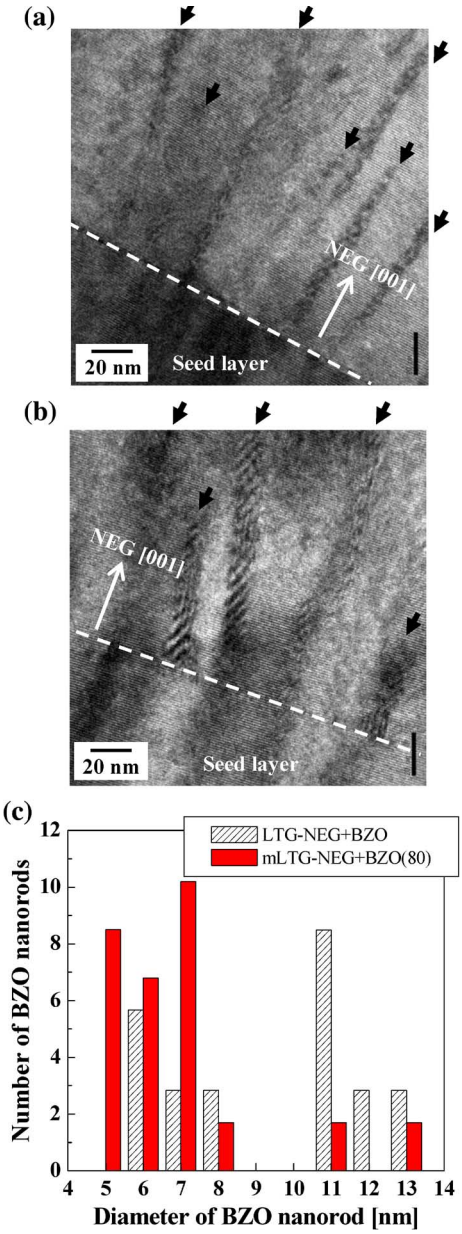

Fig. 4. Microstructure of the BZO doped films. (a) Cross sectional TEM image of the mLTG-NEG+BZO(80) film and (b) the LTG-NEG+BZO films. (c) Diameter-histogram of the BZO nanorods in the films. The number of BZO NRs was counted over in low magnification TEM images of 1 μm width.

Based on above discussion, we concluded that the increase of the BZO NRs via the introduction of BZO NDs on the surface of NEG seed layer resulted in the superior superconducting properties in the magnetic fields for the NEG+BZO film.

IV. Conclusion

In order to enhance BZO nanorods density for a further enhancement of J_c in magnetic fields, we introduced BZO into NEG films grown by LTG technique. Especially, J_c in magnetic fields was improved by an introduction of BZO nanodots on the seed layer in the LTG films. This improvement was due to a formation of the c-axis correlated pinning centers which were made of the BZO. Interestingly, the films including the BZO nanodots exhibited a remarkable enhancement of J_c. From

cross-sectional TEM observation, we confirmed that the BZO nanodots prevented a growth of a coarse BZO nanorod and the high density BZO nanorods were formed in the films.

REFERENCES

[1] M. Itoh, Y. Yoshida, Y. Ichino, M. Miura, Y. Takai, K. Matsumoto, A. Ichinose, M. Mukaida, and S. Horii, "Low temperature growth of high- J_c $Sm_{1+x}Ba_{2-x}Cu_3O_y$ films," *Physica C*, vol. 412–414, pp. 833–837, 2004.

[2] Y. Yoshida, K. Matsumoto, M. Miura, Y. Ichino, Y. Takai, A. Ichinose, S. Horii, and M. Mukaida, "High-critical-current-density $SmBa_2Cu_3O_{7-x}$ films induced by surface nanoparticle," *Jpn. J. Appl. Phys.*, vol. 44, pp. L546–L548, 2005.

[3] Y. Yoshida, Y. Ichino, M. Miura, Y. Takai, K. Matsumoto, A. Ichinose, S. Horii, and M. Mukaida, "High critical current density in high field in $Sm_{1+x}Ba_{2-x}Cu_3O_{6+y}$ thin films," *IEEE Trans. Appl. Supercond.*, vol. 15, pp. 2727–2730, 2005.

[4] M. Miura, Y. Yoshida, Y. Ichino, T. Ozaki, Y. Takai, K. Matsumoto, A. Ichinose, S. Horii, and M. Mukaida, "Dislocation density and critical current density of $Sm_{1+x}Ba_{2-x}Cu_3O_y$ films prepared by various fabrication processes," *Jpn. J. Appl. Phys.*, vol. 45, pp. L701–L704, 2006.

[5] M. Muralidhar, N. Sakai, M. Nishiyama, M. Jirsa, T. Machi, and M. Murakami, "Pinning characteristics in chemically modified (Nd, Eu, Gd)-Ba-Cu-O superconductors," *Appl. Phys. Lett.*, vol. 82, pp. 943–945, 2003.

[6] K. Inoue, Y. Yoshida, Y. Ichino, Y. Takai, K. Matsumoto, A. Ichinose, M. Mukaida, and S. Horii, "Superconducting properties in magnetic field of $(Nd, Eu, Gd)_{1+x}Ba_{2-x}Cu_3O_y$ thin films prepared by low temperature growth technique," *Physica C*, to be published.

[7] J. S. Kang, A. Goyal, J. Li, A. A. Gapud, P. M. Martin, L. Heatherly, J. R. Thompson, D. K. Christen, F. A. List, M. Paranthaman, and D. F. Lee, "High-performance high- T_c superconducting wires," *Science*, vol. 311, pp. 1911–1914, 2006.